Magnetization and Mossbauer studies of $Zn_{0.5}Co_{0.9}Fe_{1.2}Ti_{0.4}O_4$

1995 J. Phys.: Condens. Matter 7 8183

(http://iopscience.iop.org/0953-8984/7/42/014)

J. Phys.: Condens. Matter 7 (1995) 8183–8196. Printed in the UK

Magnetization and Mössbauer studies of $Zn_{0.5}Co_{0.9}Fe_{1.2}Ti_{0.4}O_4$

M R Singh and S C Bhargava

Solid State Physics Division, Bhabha Atomic Research Centre, Bombay 400 085, India

Received 1 February 1995, in final form 13 July 1995

Abstract. The AC susceptibility, zero-field-cooled and field-cooled magnetization, hysteresis and Mössbauer studies in the temperature range of 4.2 to 300 K of $Zn_{0.5}Co_{0.9}Fe_{1.2}Ti_{0.4}O_4$ are reported. The observed peak in AC susceptibility, the temperature irreversibility in magnetization and the change in coercivity with temperature are shown to be due to the presence of single-domain magnetic clusters. The temperature dependence of the magnetic hyperfine field in Mössbauer spectra indicates the absence of noncollinearity of spins even at low temperatures. The anomalous shapes of the Mössbauer spectra at higher temperatures have been found to result from the presence of ionic spin relaxation. The superparamagnetic fluctuations effect affects the Mössbauer spectrum above 260 K only.

1. Introduction

Spin-glass ordering of metallic as well as nonmetallic magnetic substances has been extensively studied (for reviews see [1–3]). In this type of ordering, ionic spin at any site possesses a definite orientation below the spin-glass ordering temperature (T_{sg}), but this orientation changes from site to site, resulting in negligible net magnetization. The absence of any long-range ordering is confirmed by the neutron diffraction method. Several metallic substances have been found to undergo spin-glass magnetic ordering as the temperature is lowered. They have been described as canonical spin glasses. The temperature dependence of the AC susceptibility of these substances shows a peak at the spin-glass ordering temperature. Furthermore, the zero-field-cooled (ZFC) and the field-cooled (FC) low-field magnetizations show a branching and the FC magnetization shows a time dependence below T_{sg}. It was easy to visualize that the long range and the oscillating nature of the RKKY interaction in metallic substances can lead to such magnetic ordering when the concentration of the magnetic ions is low. Based on this, a good understanding of spin-glass ordering has been obtained using the mean-field theories [4].

However, magnetic ordering in magnetic nonmetallic oxides results from the short-range superexchange interaction. A large number of studies of the magnetic properties of the oxides with spinel, garnet, and perovskite structures have been made using magnetization, Mössbauer spectroscopy and the neutron diffraction method. Several new phenomena in oxides have been discovered. Thus, noncollinear spin structure, spin relaxation phenomena and superparamagnetic effects have been found to be present in these oxides [5]. The interest in the study of these substances has been reactivated because some of these oxides showed peaks in the temperature dependence of AC susceptibility and the branching of the FC and ZFC magnetizations. It appears that the spin-glass phenomenon is shown by magnetic

0953-8984/95/428183+14$19.50

oxides also, even though the magnetic interactions in these substances are not due to the RKKY interactions. Surprisingly, the peak has since been found in the AC susceptibility of many oxides in which spin-glass ordering is difficult to justify and which can be well described by the theories of noncollinear spin structure. Neutron diffraction also shows the presence of a long-range ordering in these oxides. It is thus indicated that there are important differences in the behaviour of metallic and nonmetallic substances even though both show peaks in AC susceptibility and branching of field-cooled and zero-field-cooled magnetizations. Since the magnetic interaction in oxides is of a short-range character, an ion interacts with its nearest neighbours (nn) or next-nearest neighbours (nnn) only. Thus, mean-field theories of spin-glass phenomena which assume that an ion interacts with all its neighbours are not applicable in this case. For these insulator oxides, discussions which explicitly take the short-range nature of the magnetic interactions into account are relevant [6–8].

The present study is concerned with the spinel oxide $Zn_{0.5}Co_{0.9}Fe_{1.2}Ti_{0.4}O_4$ which is found to show a peak in the AC susceptibility and branching of field-cooled and ZFC magnetization at lower temperatures. We have used Mössbauer spectroscopy and magnetization measurements to extensively study the magnetic behaviour of this oxide and thus the phenomena which are responsible for the peak in AC susceptibility and the branching of the FC and ZFC magnetizations. It is found that the dominant characteristic of the oxide at such high concentrations of the diamagnetic ions is that the magnetic lattice breaks into small clusters. Each of these clusters can be weakly coupled to neighbouring clusters through an exchange path. Above a certain temperature, these clusters behave independently and can thus behave like superparamagnetic particles. Below this temperature, the clusters weakly couple to each other. These clusters suffer frustration due to differing alignment effects of the neighbouring clusters and as a result align in different directions. The ordering is somewhat similar to spin-glass ordering in metallic substances, the only difference being that in metallic substances spin-glass ordering of ions occurs, whereas in oxides the spin-glass ordering of clusters takes place. This ordering of clusters is responsible for the increase in coercivity at lower temperatures. The theoretical understanding of these effects is expected to be obtainable from the mean-field theories of metallic spin glasses. The magnetic behaviour observed is found to be due to the presence of single-ion spin relaxation and the phenomena of superparamagnetism.

2. Experimental details

The sample was prepared using the conventional ceramic technique. High-purity oxides TiO_2, Co_3O_4, ZnO and Fe_2O_3 were taken in the desired stochiometric ratio, thoroughly mixed under alcohol, and calcined at 900 °C for 36 hours. The final sintering was done at 1200 °C for 20 hours. The x-ray diffraction showed the compound formed to be a single-phase cubic spinel. The cell constant is 8.431 ± 0.001 Å.

The real and imaginary parts of the low-field AC susceptibility have been recorded using a closed-cycle refrigerator. The susceptibility has been recorded as the temperature increases.

DC magnetization studies have been made using a SQUID magnetometer (Quantum design MPMS-2). The temperature dependence of the zero-field-cooled magnetization was recorded after the sample was cooled from its paramagnetic state at 350 K to the ordered state at 5 K in zero magnetic field. The experimental field was switched on and the (ZFC) magnetization was recorded as the sample warmed up to 350 K. The sample was again cooled down to 5 K in presence of this field and the (FC) magnetization was recorded as

the temperature decreased. The external fields used for such measurements range from 0.1 to 2.5 kOe. The hysteresis loops have been obtained by cooling the sample from 350 K to the desired temperature in the zero field. The maximum field used in these measurements is ±15 kOe.

A Mössbauer spectrometer operated in the constant-acceleration mode and transmission geometry has been used to obtain spectra in the temperature range from 100 to 300 K. Another spectrometer has been used to obtain spectra at lower temperatures. In this set up, the drive waveform used is sinusoidal and both ends of the long drive rod are used to obtain spectra: one end for the sample under investigation and the other end for the Fe metal spectrum. Thus, the calibration spectrum is obtained simultaneously. The Mössbauer sources used are ^{57}Co in a *rhodium* matrix. The temperature measurement and control in the range from 100 to 300 K is done using a Cu–constantan thermocouple. At lower temperatures, a calibrated carbon glass resistance sensor is used for this purpose.

3. Results

The temperature dependencies of the real and imaginary parts of the AC susceptibility are shown in figure 1. The real part (χ') shows that the transition from the paramagnetic to the magnetic state occurs at ≈300 K. χ' shows a peak at 272 K. As will be discussed later, this peak is due to the gradual blocking of the superparamagnetic cluster fluctuations as the temperature decreases. The decrease in χ' is faster below ≈50 K. Below this temperature, the coupling between clusters due to the weak exchange bond becomes larger than the thermal energy. The effective cluster size, therefore, increases. The signal strength of the imaginary part (χ'') is very low and has not been used to obtain any information about the magnetic behaviour of the oxide.

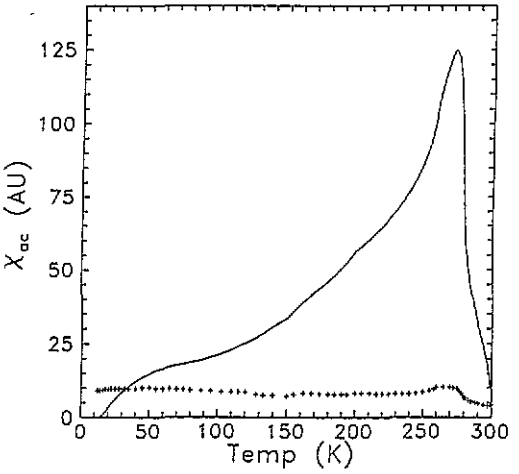

Figure 1. Temperature dependence of the real and imaginary (+) parts of AC susceptibility.

The temperature dependence of the FC and ZFC magnetizations are shown in figure 2. The FC magnetization is weakly dependent on temperature below 50 K. The branching of ZFC and FC magnetizations occurs at a temperature which depends on the magnetic field. This branching is observable even in a field of 2.5 kOe. The dependence of the magnetic field on the square root of the branching temperature of ZFC–FC magnetization is shown

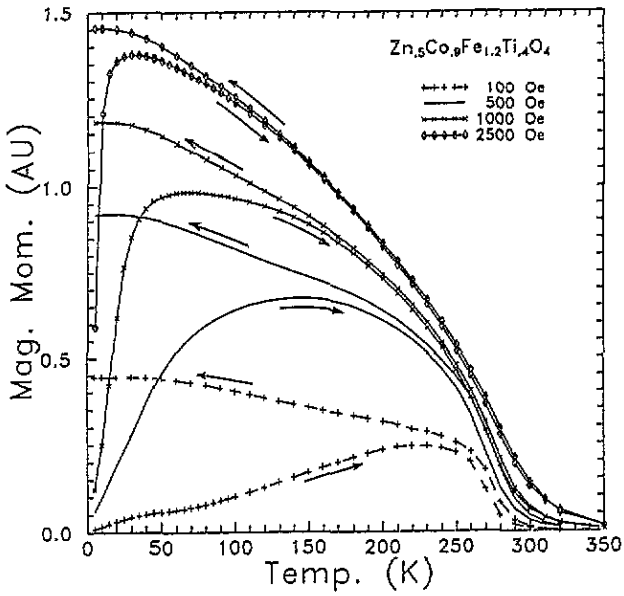

Figure 2. Temperature and field (+, 100 Oe; −, 500 Oe; ×, 1 kOe; ◇, 2.5 kOe) dependencies of FC and ZFC magnetizations.

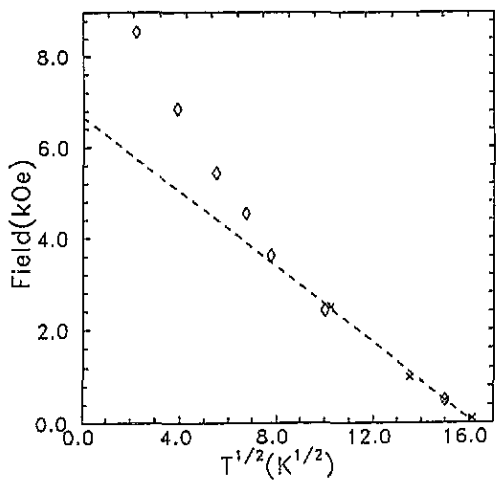

Figure 3. Branching point of the ZFC–FC magnetization (×) and the field at which the hysteresis loop closes (◇) against the square root of temperature. The linear fit (−) for $T > 60$ K is also shown.

in figure 3. The dependence in the temperature range from 60 to 225 K is linear.

The magnetic hysteresis loops have been obtained at several temperatures (figure 4). These measurements reveal three aspects of the magnetic behaviour of the oxide. Firstly, the value of the field above which the magnetization in the hysteresis loop is reversible is temperature dependent. The dependence of this field on the square root of temperature thus obtained is found to be linear at temperatures above 60 K. Secondly, the slope of the

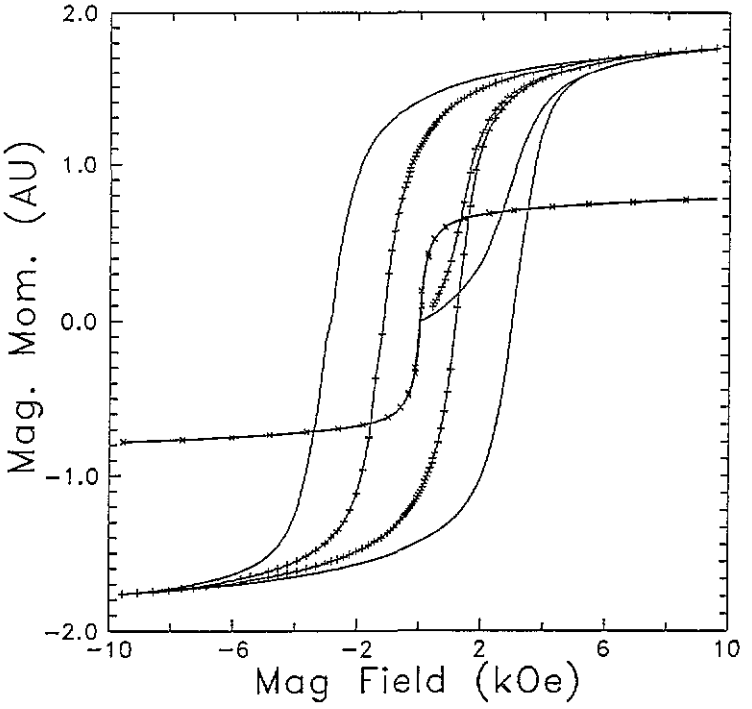

Figure 4. Typical hysteresis loops at different temperatures (−×−, 225 K; −+−, 15 K; −, 5 K).

reversible part of the hysteresis loop, in the range of field from 10 to 15 kOe, is found to be negligible at temperatures greater than 60 K. This indicates an absence of the canting of magnetic moments at temperatures greater than 60 K. As will be seen later, Mössbauer spectroscopy shows the absence of noncollinearity at lower temperatures also. Lastly, the coercive field is found to increase as the temperature decreases. The increase becomes larger at lower temperature, $T < 50$ K.

The Mössbauer spectrum at the ambient temperature is an asymmetric doublet (figure 5(*a*)). It is fitted with two symmetric doublets. The results of the analysis are given in table 1. The spectrum at 4.2 K (figure 5(*b*)), obtained using a 1024 channel analyser, shows that the two component spectra are resolved. The sixth line is sufficiently split. Furthermore, line broadening at 4.2 K due to dynamical effects is negligible. The spectrum is fitted with two symmetric sextets. This enables the determination of the area ratio of the two components to be performed. The results of the analysis are also included in table 1. There is a good agreement between the ratio of the areas of the two component spectra obtained from the spectra at 4.2 K and the ambient temperature. In the cubic spinel structure of the oxide, the unit cell contains two types of inequivalent cationic site, known as A and B sites, which possess a tetrahedral and octahedral coordination of the oxygen ions, respectively. The two components in the Mössbauer spectra correspond to these inequivalent sites. The component spectra can be resolved with better accuracy provided the spectrum is recorded at ≈4.2 K in the presence of an external magnetic field. This is essential for finding the correct site occupancy of iron [9]. However, using the fact that Zn^{2+} and Ti^{4+} prefer A and B sites respectively, the cation distribution can be concluded to be

$$(Zn_{0.5}Fe_{0.5})[Co_{0.9}Fe_{0.7}Ti_{0.4}]O_4.$$

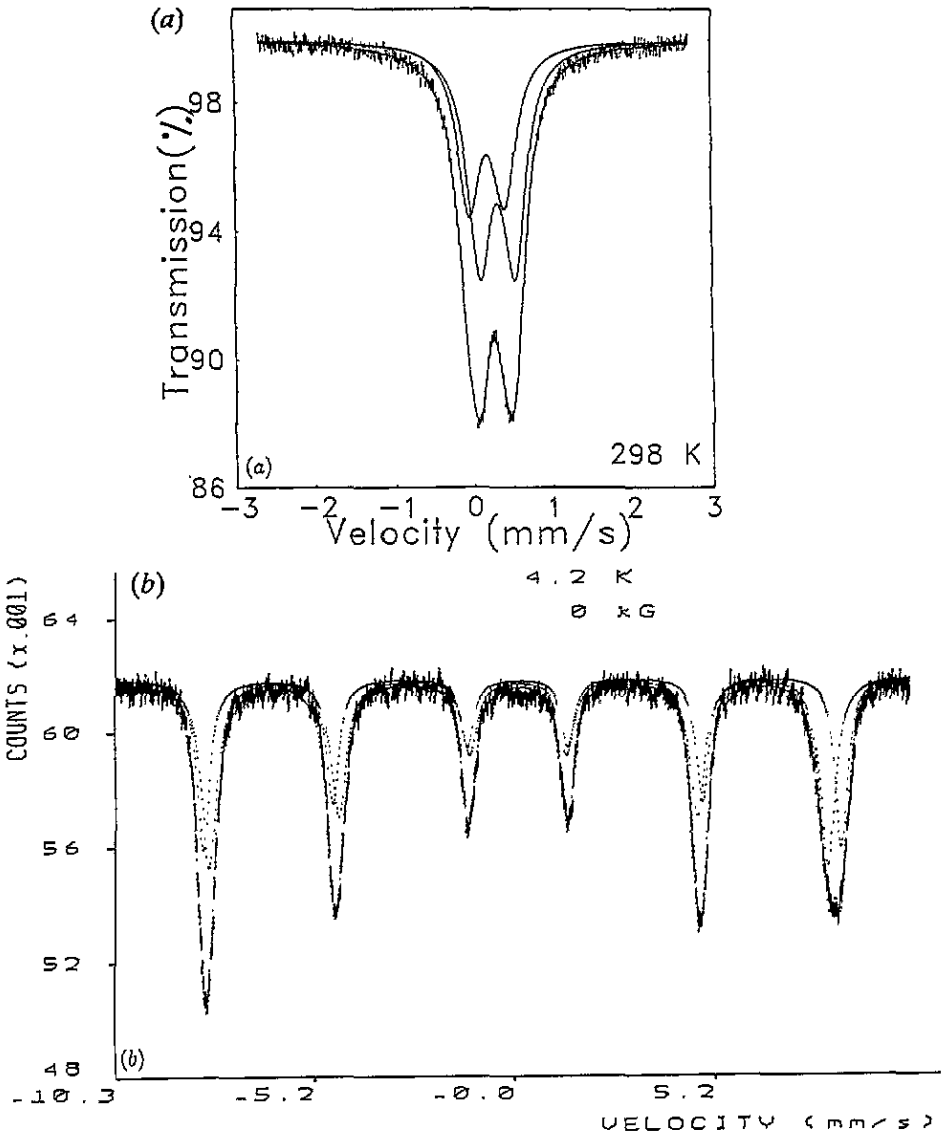

Figure 5. Mössbauer spectra (*a*) at 298 K and (*b*) at 4.2 K.

The hyperfine fields and isomer shifts which characterize the two component spectra show that iron is in a high-spin Fe^{3+} state.

As the temperature increases, the lines in the Mössbauer spectrum start broadening. Thus, even at 20 K, it becomes difficult to resolve the spectrum into two sextets without using constraints. As the cation distribution is expected to be temperature independent, the ratio of the areas of the two sextets has been constrained to be 5:7 to fit the spectra at higher temperatures. The sextets were assumed to be symmetric, but the lines of the two sextets were allowed to differ in width. This is a reasonable assumption in view of the possibility that the two component spectra can have different dynamical effects, which is responsible for line broadening in the present case. The temperature dependence of the

Table 1. Results of analyses of Mössbauer spectra.

Temperature (K)	Site	Centre shift† (mm s^{-1})	Quadrupole split‡ (mm s^{-1})	Magnetic field (kOe)	Relative intensity (%)
298	A	0.265 ± 0.011	0.459 ± 0.003	—	42 ± 7
	B	0.392 ± 0.008	0.453 ± 0.004	—	58 ± 8
4.2	A		0.19 ± 0.01	518.7 ± 2.3	43 ± 7
	B		-0.04 ± 0.003	503.1 ± 2.1	57 ± 8

† Centre shifts are relative to the centre of the Fe metal spectrum.
‡ QS represents δ_{12} for the paramagnetic spectrum and $\delta_{12} - \delta_{56}$ for the magnetic sextet.

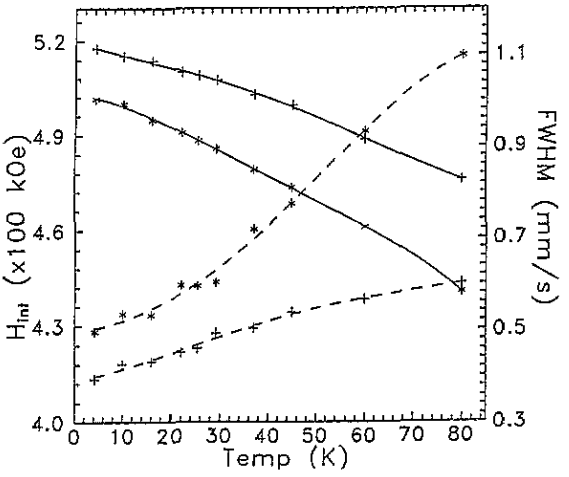

Figure 6. Temperature dependence of hyperfine fields (−) and line widths (- -) for site A (+) and site B (∗).

line widths and the hyperfine fields thus obtained are shown in figure 6. The line widths increase with temperature. The change with temperature is, however, different for the two components. The temperature dependence of the hyperfine fields show no anomaly. This is different from the anomaly found in $Ni_{0.25}Zn_{0.75}Fe_2O_4$ [12], Mg–Ti [10] and Li–Ti ferrites [11] which were found to be related to the change of noncollinear to collinear structure. The absence of an anomaly in the present case, therefore, implies an absence of noncollinearity in $Zn_{0.5}Co_{0.9}Fe_{1.2}Ti_{0.4}O_4$ even at low temperatures (up to 4.2 K).

At higher temperatures, the line shape becomes anomalous. It is characterized by larger line width and an increase in δ_{16}/δ_{34} with temperature. Here, δ_{ij} denotes the separation between the ith and jth lines in the Mössbauer spectrum. This indicates the presence of single-ion spin relaxation effects on the Mössbauer spectra, as has been found in several other samples earlier [12]. The difference in temperature dependences of the line widths of the two component spectra in the temperature range from 4.2 to 80 K (figure 6) mentioned above indicates different temperature dependence of the relaxation times also. For this reason, the experimental spectra have been fitted with two theoretically simulated relaxation spectra. The relative areas of the two components have been constrained to the values found at 4.2 K. In the present case, the relaxation occurs in the presence of the Weiss exchange field and thus an adiabatic approximation is valid. For this adiabatic case, the procedure

for the simulation of the line shapes using the stochastic model of ionic relaxation has been described in detail elsewhere [12, 13]. The line shape corresponding to a nuclear transition is given by

$$I(w) = -\frac{2}{\Gamma}\mathrm{Re}\{\boldsymbol{W}\mathbf{A}^{-1}\mathbf{1}\} \tag{1}$$

where $\boldsymbol{W} = \{s^5, s^4, s^3, s^2, s, 1\}$ is a row vector, s denotes the ratio of thermal population of the successive ionic Zeeman levels, $\mathbf{1}$ is the unit column vector and $\mathbf{A}$ is a 6×6 matrix which depends on the value of the hyperfine field ($H_{int}(0)$), the line width in the absence of relaxation is Γ and the spin–spin relaxation rates Ω_{ss} [12, 13]. At low temperatures, spin–lattice relaxation rates are small and are therefore neglected. All the parameters except s and Ω_{ss} are obtainable from the spectrum at the lowest temperatures, where relaxation effects are necessarily negligible. As described elsewhere [12, 13], the relaxation time is given by

$$\tau = \frac{1}{7(1+s)\Omega_{ss}} \tag{2}$$

and the ionic magnetization is related to the s parameter by

$$\langle S_z \rangle = \frac{2.5 + 1.5s + 0.5s^2 - 0.5s^3 - 1.5s^4 - 2.5s^5}{1 + s + s^2 + s^3 + s^4 + s^5}. \tag{3}$$

In fitting the experimental spectra, s and Ω_{ss} have been treated as the variable parameters. The theoretical spectra which have the best fits with the experimental spectra at various temperatures are shown with solid lines in figure 7. Thus, we can fit the experimental data at temperatures lower than 260 K with only two adjustable parameters: the relaxation time and the ionic magnetizations. The temperature dependences of these two parameters are shown in figure 8.

It is even visually clear (figure 7) that a paramagnetic component develops and coexists with the magnetic component at higher temperatures ($T > 260$ K). The relative intensity of the paramagnetic component increases with temperature. The complete conversion of the magnetic spectrum into the paramagnetic doublet occurs in a narrow range of temperature. In this range of temperature, we fit the experimental spectrum with two magnetic spectra affected by single-ion relaxation and a paramagnetic doublet due to fast fluctuating clusters. The relaxation times of the paramagnetic doublet thus obtained at two different temperatures are shown in figure 8.

4. Discussion

In oxides with a high concentration of diamagnetic ions, as in the present case, the number of broken magnetic paths becomes large. As the magnetic interaction is due to the superexchange short-range interactions, the magnetic lattice starts breaking into small clusters [15]. At higher temperatures, superparamagnetic fluctuation times of these clusters become smaller than the characteristic time of measurement. This gives a peak in AC susceptibility and a splitting of the Mössbauer spectrum into a magnetic and a paramagnetic component. The peak in the AC susceptibility at 270 K shows that the superparamagnetic blocking temperature of the single-domain magnetic clusters is, on average, 270 K. The appearance of a well defined peak further shows that the sizes of the clusters, and therefore the blocking temperatures of these clusters, do not vary much from cluster to cluster.

Each of these clusters is weakly coupled to neighbouring clusters through an exchange path. The shoulder in the real part of χ_{ac} at temperatures of around 50 K shows that the

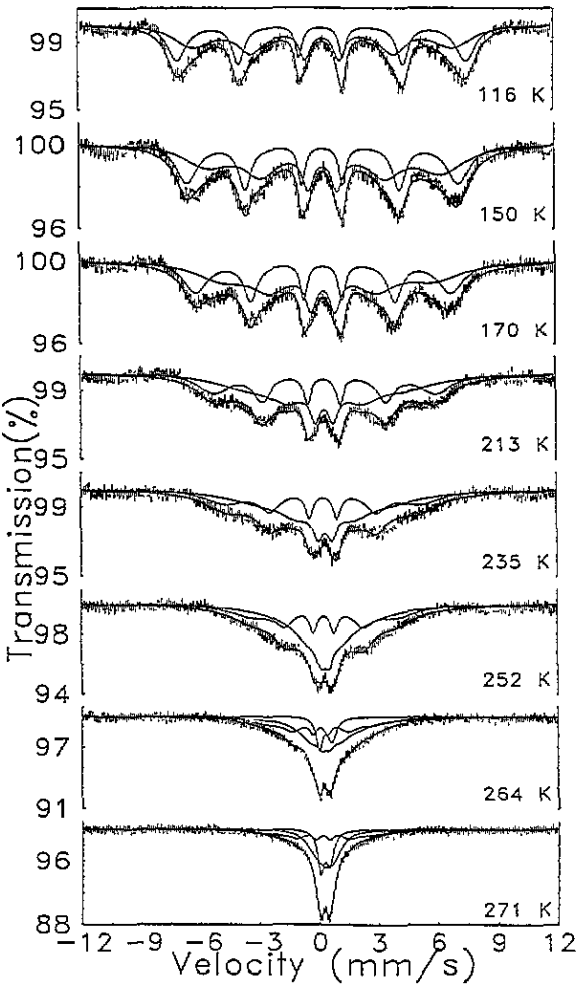

Figure 7. Mössbauer spectra in the temperature range 100–270 K fitted by the stochastic ionic spin relaxation method.

strength of the exchange coupling between clusters is ≈4.3 meV. Above this temperature, clusters behave independently, although superparamagnetic fluctuations set in at much higher temperatures of around 270 K. Below 50 K, the exchange coupling between clusters becomes greater than the thermal energy, resulting in an increase in the effective volume of the clusters at a lower temperature. Furthermore, the different neighbouring clusters tend to align the magnetization of the central cluster in different directions. This leads to a frustration. As a result, different clusters align in different directions. The situation is similar to spin-glass ordering in metallic substances, with the difference that in the metallic substances spin-glass ordering of ions occurs, whereas in the oxides spin-glass ordering of the clusters takes place. A multiple-domain structure does not form in either case.

The branching of the FC and ZFC magnetizations can also occur due to the phenomena of superparamagnetism as follows. When the field is applied at a temperature above the blocking temperature, we obtain FC magnetization, which has a reversible temperature dependence. On the other hand, if the sample is cooled to a temperature below the

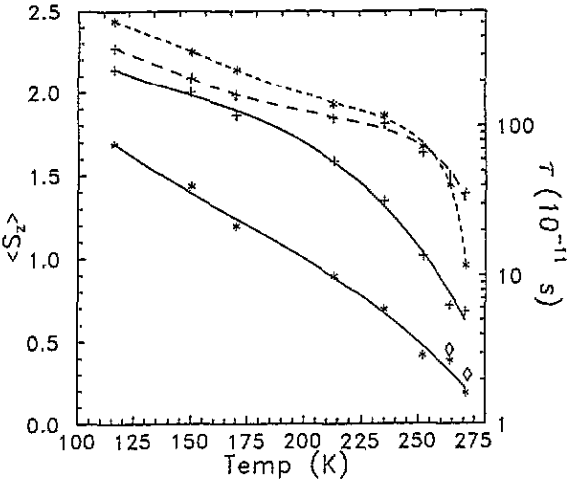

Figure 8. Temperature dependence of ionic spin ($\langle S_z \rangle$) (—) and relaxation time (τ) (- -) for site A (+) and site B (*). The relaxation time for the paramagnetic component (◇) is also shown.

blocking temperature (5 K in the present experiment) before applying the external field, the coercive force prevents the magnetization from reaching the equilibrium value. The effect of the coercive force disappears only when the temperature is increased back to the blocking temperature and the ZFC magnetization coincides with the FC magnetization. Thus, the branching point of the FC and ZFC magnetizations is a measure of the blocking temperature. Larger clusters have larger blocking temperatures. Unless the external field is applied at a temperature above the blocking temperature of all the clusters, reversible FC magnetization behaviour is not obtained. Thus, the branching temperature represents the blocking temperature of the largest cluster [16].

Furthermore, the external field lowers the blocking temperatures of clusters, and therefore the branching temperature (T_B) is lower in presence of a higher external field. The dependence of the blocking temperature on field can be easily obtained. The potential energy barrier in the absence of the field is κV and the barrier in the presence of the field H is $\kappa V - \mu H + (\mu H)^2/4\kappa V$, where κ is the magnetic anisotropy constant, V is the volume and μ the magnetization of the cluster. The ratio $T_B(H)/T_B(H=0)$ is related to the field, denoted by H_B, by the equation [16, 17]

$$H_B = \frac{2\kappa V}{\mu}\left[1 - \left(\frac{T_B(H)}{T_B(H=0)}\right)^{\frac{1}{2}}\right]. \tag{4}$$

In figure 3, the field H_B is plotted against the square root of the branching temperature. It can be fitted by a straight line at temperatures above 60 K. The intercept of this curve on the field axis gives $2\kappa V/\mu$. At lower temperatures, coupling between clusters also becomes important, which leads to an increase in the effective volume V of the cluster and hence, as equation (4) shows, the slope of the straight line is expected to increase at lower temperatures. This is also manifested by a larger coercivity field at lower temperatures. The coercive field referred to in the above discussion of branching of magnetizations is, however, different from the coercivity field measured in the hysteresis loop measurement. In the temperature dependence of the FC and ZFC magnetizations, the coercive force of the largest cluster corresponds to the branching point [16]. In the hysteresis loop the coercivity

field corresponds to the average of all the clusters. Nevertheless, the coercive field obtainable from the hysteresis loop is also expected to show an increase at lower temperatures due to the increase in the effective volume of the clusters. This is indeed obtained (figure 4).

In the present case, the irreversibility in the hysteresis loop is not due to the presence of a multi-domain structure but to coercive forces of the clusters. The field above which the hysteresis loop becomes reversible, denoted by (H_B), is also related to the blocking temperature of the largest cluster in the following way. The hysteresis curve is reversible at all fields when the temperature is greater than the blocking temperature in zero field, $T > T_B(H = 0)$. The area of the loop is therefore zero. At temperatures below $T_B(H = 0)$, the field dependence of the blocking temperature (equation (4)) is to be considered. When the field in the hysteresis loop measurement is such that the anisotropy energy barrier of the cluster is greater than the thermal energy, $T_B(H) > T$, the magnetization is irreversible. As the field increases, the barrier decreases and eventually becomes equal to the thermal energy, $T = T_B(H)$. This field is denoted by H_B. At higher fields, $H > H_B$, the barrier is less than the thermal energy and consequently the magnetization is reversible. Thus, for the field H_B at which the irreversible and reversible part of the loop join, $T = T_B$. The hysteresis loops at various temperatures enable the determination of several pairs of H_B and $T_B(H_B)$ to be performed. The dependence of H_B on the square root of $T_B(H_B)$ obtained from these measurements shows a good agreement with the dependence obtained from the branching point of the FC and ZFC magnetizations shown in figure 3.

Mössbauer spectroscopy measurements at several temperatures in the range from 4.2 K to 300 K have revealed several interesting features. The temperature dependence of the hyperfine fields at low temperatures has been obtained in order to determine the anomaly at the temperature at which the noncollinear structure is converted into a collinear structure [10–12]. Such an anomaly was found earlier in the case of oxides which show a noncollinearity at low temperatures [10–12]. In the present case no such anomaly is found which therefore implies absence of noncollinearity in the spin structure around the Mössbauer probe even at low temperatures.

Such an anomaly has been found in the temperature dependence of the hyperfine field in the case of re-entrant spin glass AuFe also, though its characteristics are remarkably different, particularly the field dependence [18–20]. In oxides, the temperature dependence of the hyperfine field is very sensitive to the field, and the anomaly rapidly disappears as the field increases [12]. In metallic substances, the shape of the anomaly is not affected by the external field. Its origins in oxides and metallic substances are, therefore, expected to be very different.

The increase in temperature results in line broadening in the Mössbauer spectra. This line broadening is appreciable even at 20 K. At higher temperatures, the shape becomes anomalous. Such anomalous line shapes can be fitted by assuming either the presence of the ionic spin relaxation effects or a distribution of hyperfine interaction parameters. There are different reasons for preferring one method of fitting over the other.

It is well known that diamagnetic ions can occupy any cationic site randomly. Therefore, the magnetic environment around each Fe^{3+} ion can vary from site to site. There are two ways in which this can affect Mössbauer spectra. Firstly, this can give a variation in the saturation hyperfine fields through supertransferred hyperfine interaction [21]. This is, however, not found. The spectrum at 4.2 K shows two sextets corresponding to the A and B sites only, and the lines in the sextets are sharp. Alternatively, the temperature dependence of $\langle S_z \rangle$ can be strongly influenced by the neighbourhood. As the number of possible near-neighbour configurations which have a significant probability of existence is small, the number of component sextets required to fit the broadened shapes should be

small. In this case, it is reasonable to expect that the broadened line shapes should split into component sextets at some temperature at least. Experimentally, however, even though the spectra of all mixed ferrites investigated so far have shown these broadened shapes, in no case is there even a hint of a structure appearing. The shortcomings of an interpretation based on a distribution of hyperfine fields in magnetic oxides have been discussed in [21]. It therefore appears that this is not the correct interpretation of the anomalous shapes even though this mode of fitting provides enough flexibility to fit almost any broad line shape.

It is to be emphasized that the validity of this mode of analysis, however, requires an absence of the relaxation effect. In the presence of relaxation effects, the hyperfine field alone does not govern line separations and widths.

The presence of relaxation effects is strongly indicated by the increase in δ_{16}/δ_{34} with the increase in temperature. Further support is provided by the very reasonable temperature dependence of τ and $\langle S_z \rangle$ obtained by fitting the spectra at various temperatures. Furthermore, the spectra at different temperatures can be fitted by varying only two parameters. Anomalous shapes have been found in the Mössbauer spectra of all the magnetic oxides with appreciable concentrations of the diamagnetic cations. In all these cases, δ_{16}/δ_{34} has been found to increase with temperature. The analysis of the shapes using the stochastic model of single-ion relaxation has been successful in all cases. This further supports such a mode of analysis in the present case also [12, 13, 15].

At higher temperatures, in addition to the single-ion relaxation, superparamagnetic (SPM) fluctuation affects the Mössbauer spectra. This phenomenon has been found earlier in other ferrites with an appreciable concentration of the diamagnetic ions, even though the physical size of the grain is not small. This division of the magnetic lattice into a cluster is due to the presence of the diamagnetic ions and the short-range nature of the exchange interaction which are responsible for the magnetic ordering in oxides. The exponential dependence of the SPM fluctuation rates on $\kappa V/k_B T$ results in a rapid change in the fluctuation rate with temperature. When the superparamagnetic fluctuations of a cluster become faster than the nuclear precession period of the Mössbauer ion, the magnetic Mössbauer spectrum originating from ions in this cluster collapses into a paramagnetic component. Thus, magnetic splitting collapses rapidly as the temperature increases. When clusters of different sizes are present, the collapse of spectra originating from different clusters occurs at different temperatures. In this range of temperature, magnetic and paramagnetic spectra coexist, and the relative intensity of the paramagnetic component increases with temperature. In some cases, the temperature range over which the conversion takes place is found to be large [14, 15], in other cases, this occurs in a narrow range of temperature. The present measurements show that the blocking temperatures of various clusters in the oxide under study lie in a narrow range of temperature. The process of conversion of the magnetic spectra into the paramagnetic component occurs rapidly in the range of temperature from 260 to 300 K and is completed before 300 K, at which temperature the entire spectrum is paramagnetic. The peak in the AC susceptibility at 270 K is related to these superparamagnetic fluctuations. The sharpness of the peak is also related to the narrow range of temperature over which the collapse of the magnetic splitting of the Mössbauer spectrum occurs.

These fluctations are different from the single-ion relaxation which is present at lower temperatures. An important distinction between the two is that whereas the spin–spin relaxation rate is independent of temperature, the superparamagnetic fluctuation depends exponentially on T^{-1}. Thus, the spin–spin relaxation rate is large even at low temperatures and the effect is thus present even at low temperatures. The superparamagnetic fluctuations, on the other hand, have an effect at higher temperatures only and, unless the distribution

in particle size is large, affect the spectrum in a very narrow range of temperature. When κV starts becoming comparable to the thermal energy $k_B T$, the fluctuations become rapid and more important than the single-ion relaxation, leading to the collapse in the magnetic splitting.

5. Conclusions

In oxides with large concentrations of diamagnetic cations, the magnetic lattice consists of weakly exchange-coupled clusters. At a temperature lower than that required for exchange coupling between clusters, the effective cluster size becomes large and results in a rapid increase in coercivity as the temperature is lowered below 50 K. At higher temperatures, $T > 60$ K, these clusters behave independently. The superparamagnetic fluctuation time of these clusters, however, becomes smaller than the characteristic measurement time above 260 K only. This results in a peak in AC susceptibility at 270 K and the splitting of magnetic Mössbauer spectrum into paramagnetic and magnetic components over this range of temperature. In the present case, the AC susceptibility peak is sharp, indicating that the cluster sizes fall in a narrow range. Mössbauer spectra also show that the variation in the cluster size is small. In several other oxides, however, this variation in cluster size is found to be large [14, 21], which results in a broader AC susceptibility peak as well as a large range of temperature over which the Mössbauer spectrum shows coexistence of paramagnetic and magnetic components. The branching temperature of the FC and ZFC magnetizations is equal to the blocking temperature of the largest cluster corresponding to the external field. The two are therefore related by equation (4). In the measurement of the hysteresis loop at any temperature T, the magnetization becomes reversible from irreversible beyond a certain value of field. This field and the temperature are also related by the relation (4), due to the phenomena of superparamagnetic fluctuations. Data thus obtained from both these measurements show good agreement, and support our interpretation. It is thus found that the peak in the AC susceptibility and the branching of the FC and ZFC magnetizations are related to the phenomena of superparamagnetic fluctuations. The results are in agreement with the conclusions arrived at in [14, 21].

This is in addition to the locally canted structure [6] inside any cluster which can appear due to the presence of the diamagnetic ions. Mössbauer spectra, however, do not show the anomaly in the temperature dependence of hyperfine fields which accompanies the appearance of noncollinearity at low temperatures [7]. The broadened Mössbauer spectra at all temperatures have been successfully analysed using the ionic spin relaxation.

Acknowledgments

We are indebted to Shri T V Chandrasekhar Rao for help in recording the data on the SQUID magnetometer and Shri R Ganguly for the recording of AC susceptibility.

References

[1] Binder K and Young A P 1986 *Rev. Mod. Phys.* **58** 801
[2] Fisher K H 1983 *Phys. Status Solidi* b **116** 357; 1985 *Phys. Status Solidi* b **130** 13
[3] Huang C Y 1985 *J. Magn. Magn. Mater.* **51** 1
[4] Gaby M and Toulouse G 1981 *Phys. Rev. Lett.* **47** 201
[5] Dorman J L and Nogues M 1990 *J. Phys.: Condens. Matter* **2** 1223
[6] Rosencwaig A 1970 *Can. J. Phys.* **48** 2857, 2868

[7] Villain J 1979 *Z. Phys.* B **33** 31
[8] Scholl F and Binder K 1980 *Z. Phys.* B **39** 239
[9] Vandenberghe R D and De Grave E 1989 *Mössbauer Specroscopy Appled to Inorganic Chemistry* ed G J Lojg and F Grandjean F (New York: Plenum) p 59
[10] Brandt R A, George-Gibert H, Hubsch J and Heller J 1985 *J. Phys. F: Met. Phys.* **15** 1987
[11] Dormann J L, El Harfaoui M, Nogues M and Jové *J 1987 J. Phys. C: Solid State Phys.* **20** L167
[12] Bhargava S C and Zeman N 1980 *Phys. Rev.* B **21** 1717, 1726
[13] Iyenger P K and Bhargava S C 1971 *Phys. Status Solidi* b **46** 117
[14] Singh M R and Bhargava S C 1994 *Solid State Commun.* **90** 183
[15] Bhargava S C, Mulder F M, Thiel R C and Kulshreshtha S K 1990 *Hyperfine Interact.* **54** 459
[16] Candela G A and Harris R A 1979 *Appl. Phys. Lett.* **34** 868
[17] Bean C P and Livingstone J D 1959 *J. Appl. Phys.* **30** 120S
[18] Campbell I A, Senoussi S, Verret F, Teillet J and Hamzic A 1983 *Phys. Rev. Lett.* **50** 1615
[19] Lange S, Abd-Elmeguid M M and Micklitz H 1990 *Phys. Rev.* B **41** 6907
[20] Meyer C, Hartmann-Boutron, Gros Y and Campbell I A 1985 *J. Magn. Magn. Mater.* **46** 254
[21] Bhargava S C and Iyengar P K 1974 *J. Physique Coll.* **35** C6 669